70% POWER CONVERSION EFFICIENCY AL-FREE DIODE LASER BAR

M. Kanskar*, Z. Dai, T. Earles, D. Forbes, T. Goodnough, M. Nesnidal, and E. Stiers
Alfalight, Inc.
1832 Wright St
Madison, WI 53704
mkanskar@alfalight.com

D. Botez and L. J. Mawst
University of Wisconsin-Madison
1415 Engineering Dr
Madison, WI 53706

ABSTRACT

Al-free active diode laser emitting near 970 nm wavelength has been optimized for high electrical-to-optical power conversion efficiency. There are numerous key contributors such as scattering and absorption losses, band alignment, Joule heating, carrier leakage and below-threshold losses that contribute to power loss mechanisms. We report on improvement from 50% to a record high 70% power conversion efficiency on a 1 cm bar at 25C resulting from multi-pronged approach that has been taken to minimize each of the loss mechanisms to improve the overall power conversion efficiency.

1. INTRODUCTION

High power diode lasers emitting in the range of 0.8 µm to 1.06 µm have been extensively used for pumping high power solid-state lasers such as the thin disk, slab, heat capacity and fiber lasers that are potential high-energy sources for tactical use. Use of diode lasers for pumping high-efficiency alkali- vapor lasers have also been suggested. Additionally, these pump lasers are the workhorse for erbium doped fiber amplifiers, dual-clad fiber lasers, solid-state lasers that are used in power-hungry military, medical, printing and industrial applications. Diode pumped high energy lasers (HELs) are expected to produce in excess of 100 kilowatts of power. Since the commercially available diode lasers have a typical power conversion efficiency (PCE) of 50% and solid-state materials have optical-to-optical power conversion efficiency of 20%, a total of megawatt of waste heat is not unexpected in these HEL systems. The required power supply and thermal management system for handling these high power levels make HEL systems prohibitively cumbersome and expensive. Improvement in power conversion efficiency can have far-reaching implications including lower cost, portability and improved reliability ultimately enabling HEL systems with output powers in the range of multi kilowatts to hundreds of kilowatts.

Al- free active diode lasers, i.e. InGaAs(P)/InGaP/GaAs have superior power-conversion efficiency[1] compared to conventional Al-containing devices due to their low differential series resistance[2] and higher thermal conductivity. The use of InGaAsP-based material system as opposed to InGaAs/AlGaAs material system, allows for the possibility of using strain-compensated quantum wells for better performance and higher reliability[3, 4]. A lower surface-recombination velocity of Al- free diodes leads to lower facet temperature and, in conjunction with the broadened waveguide design, record high internal optical power density at catastrophic optical mirror damage (COMD) of 18.5 MW cm^{-2} has been achieved[5]. Low reactivity to oxygen provides high quality, defect-free regrowth in Al-free material system allowing buried structures that act as lateral current confinement and index guide leading to further improvement in power conversion efficiency.

2. GROWTH & LASER DESIGN

A schematic of the conduction band edge of Alfalight's typical multimode Al-free broad waveguide diode laser is shown in Figure 1. The structure comprises InGaAs quantum well, 1.3um thick InGaAsP separate confinement heterostructure, 1um thick InGaP cladding layers and a 0.15um thick p^+-GaAs cap layer. Typical multimode Fabry Perot lasers of incoherent arrays were made on a 1 cm long bar with 100um wide apertures. Subsequently, p- and n-side metal contacts were deposited and annealed.

A broad waveguide design was used. The reason for this was twofold. Firstly, the broad waveguide design provided a large transverse effective

Report Documentation Page

Form Approved
OMB No. 0704-0188

1. REPORT DATE	2. REPORT TYPE	3. DATES COVERED
00 DEC 2004	**N/A**	**-**

4. TITLE AND SUBTITLE	5a. CONTRACT NUMBER
70% Power Conversion Efficiency Al-Free Diode Laser Bar	5b. GRANT NUMBER
	5c. PROGRAM ELEMENT NUMBER
6. AUTHOR(S)	5d. PROJECT NUMBER
	5e. TASK NUMBER
	5f. WORK UNIT NUMBER
7. PERFORMING ORGANIZATION NAME(S) AND ADDRESS(ES) **Alfalight, Inc. 1832 Wright St Madison, WI 53704; University of Wisconsin-Madison 1415 Engineering Dr Madison, WI 53706**	8. PERFORMING ORGANIZATION REPORT NUMBER
9. SPONSORING/MONITORING AGENCY NAME(S) AND ADDRESS(ES)	10. SPONSOR/MONITOR'S ACRONYM(S)
	11. SPONSOR/MONITOR'S REPORT NUMBER(S)

12. DISTRIBUTION/AVAILABILITY STATEMENT
Approved for public release, distribution unlimited

13. SUPPLEMENTARY NOTES
See also ADM001736, Proceedings for the Army Science Conference (24th) Held on 29 November - 2 December 2005 in Orlando, Florida. , The original document contains color images.

14. ABSTRACT

15. SUBJECT TERMS

16. SECURITY CLASSIFICATION OF:			17. LIMITATION OF ABSTRACT	18. NUMBER OF PAGES	19a. NAME OF RESPONSIBLE PERSON
a. REPORT	b. ABSTRACT	c. THIS PAGE			
unclassified	**unclassified**	**unclassified**	**UU**	**5**	

spot size, d/G; where d is the quantum well thickness and G is the optical confinement factor, resulting in lower optical density at the facet. Secondly, most of the optical field was confined to the waveguide layer resulting in a very small overlap of the field with the doped cladding layers leading to low free-carrier losses. As a result, a low internal loss coefficient, a_i of less than 1 cm^{-1} was obtained. This low internal loss provides a high external differential quantum efficiency, h_{ext} = 85% for 1mm long, 3% & 95% coated devices. Diode lasers with 2mm cavity length routinely achieve a slope efficiency of 1 W/A. The transverse farfield measures 35° at FWHM and the lateral farfield measures less than 7° at FWHM. The laser bar was mounted on micro-channel cooled copper heatsink.

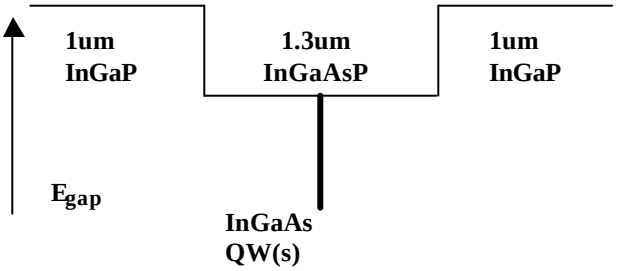

Figure 1 A schematic representation of the conduction band for an Al-free, broad waveguide 970nm diode laser transverse structure.

The laser structures were grown by low-pressure MOCVD on (100) oriented GaAs substrates. InGaAsP is typically grown in the temperature range of 610-750°C. The growth temperature selection depends on the material composition requirements. For InGaP, it is well known[6, 7] that the band-gap has a U-shaped dependence on growth temperature. InGaP displays various degrees of Cu-Pt type atomic ordering depending on epitaxial growth parameters such as temperature, V/III ratio, and substrate orientation. Ordered InGaP has a lower bandgap than disordered material by as much as 100meV. TEM studies have identified a rich microstructure in InGaP, dominated by a domain structure that is controlled by the epitaxy conditions. It has been shown that by optimizing the order-domain size, enhanced laser performance is obtained in materials that demonstrate order-disorder behavior[8].

Power losses in these diode lasers arise due to various contributing factors such as scattering and absorption losses, band alignment, Joule heating, carrier leakage and below-threshold losses. These loss mechanisms are briefly described below.

Below threshold: A certain amount of the drive current is consumed simply to attain population inversion in the laser, i.e. to get it to a threshold above which additionally injected carriers produce laser light. Further, there are non-radiative mechanisms that consume carriers.

Band alignment: The diode laser must overcome the voltage deficit resulting from misalignment of the band structure of various heterostructure interfaces. Until the deficit is overcome, useful optical power cannot be generated.

Carrier leakage: This refers to electrons and holes that do not make it to the quantum well to effectively produce photons.

Scattering and absorption: This accounts for generated photons that do not stay in the waveguide due to scattering that occurs within the quantum well, waveguide or imperfect mirrors. Additionally, photons in the waveguide can be absorbed by the free-carriers.

Joule heating: This results from the effective series resistance of the diode, which includes contact resistances as well as bulk resistance in the heterostructure itself leading to I^2R loss.

We have estimated the power losses for a 20% fill- factor diode laser bar operating at CW output power of 60 W for the plot shown in Figure 2.

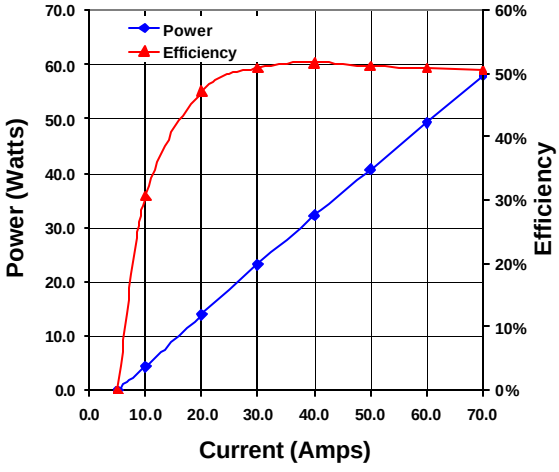

Figure 2 Plot showing typical P-I and power conversion efficiency of 970nm 1cm bar at 25C heatsink temperature.

Various losses that arise in this design are shown in the pie chart in Figure 3. A multi-pronged approach has been taken to minimize each of the loss mechanisms to improve the overall power conversion efficiency.

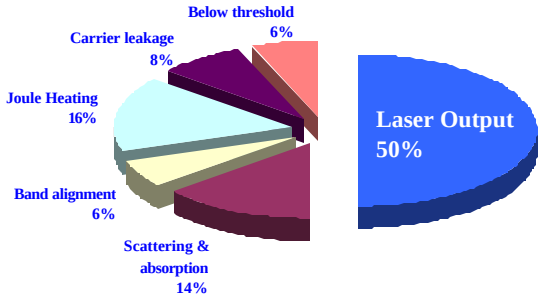

Figure 3 Power budget for a 970nm laser diode bar with 60 watt CW output, showing the relative contribution of various loss mechanisms to the overall power conversion efficiency.

3. POWER CONVERSION EFFICIENCY

The expression for the maximum power conversion efficiency, $h_{p,,max}$, is given by[1, 9]:

$$h_{p,\max} \cong h_{ext} \frac{V_F}{V_o}\left(1-2\sqrt{R_s I_{th}/V_0}\right) \qquad (1)$$

where, h_{ext} is the external differential quantum efficiency (DQE), V_F is the quasi-Fermi level difference, and V_0 is the overall built-in voltage, R_s is the series resistance and I_{th} is the threshold current. It is apparent that the four key means for improving $h_{p,max}$ are: (1) Maximizing h_{ext} (2) Minimizing V_0 (3) Minimizing R_s, and (4) Minimizing I_{th}. In a CW operation, h_{ext} is a function of temperature and is given by:

$$h_{ext}(T) = h_{ext}(T_h)\exp\left(-\frac{\Delta Tj}{T_1}\right) \qquad (2)$$

where T_h is the heatsink temperature, and DT_j is the junction-temperature rise (i.e., $T = T_h + DT_j$), and T_1 is the characteristic temperature coefficient for h_{ext}. Since V_0 is weakly dependent on temperature, the temperature dependence of $h_{p,max}$ is primarily determined by the temperature dependence of h_{ext}. Therefore, it is of paramount importance to improve the thermal properties of diode laser by maximizing T_1, and minimizing DT_j.

As shown in Equation (1) increase in h_{ext} and reduction in V_0 will have the most significant impact on peak power conversion efficiency. We will report on current status of improving these two factors. In the future we will report on optimization of series resistance and threshold current.

4. EFFICIENCY OPTIMIZATION

It is clear from Equation (1) that maximum power conversion efficiency is directly proportional to external differential quantum efficiency which, in turn, is proportional to $?_i$, injection efficiency, as shown in Equation (3) where a_m is mirror loss and a_i is all the internal loss.

$$h_{ext} = h_i \frac{a_m}{a_m + a_i} \qquad (3)$$

From our production Al-free active broad waveguide laser structure at 970 nm we routinely achieve an internal injection efficiency of 90%. It has been previously shown[10] that the use of strained barriers can reduce active region carrier leakage. This can be understood as illustrated in Figure 4. Introducing strain in the barriers lead to heavy-hole and light-hole splitting. As a result, effective barrier height for the holes becomes larger thus suppressing hole leakage. We have optimized the strain-thickness product of the quantum well barriers and shown that for a value of approximately 5%-nm, the calculated internal injection efficiency improves to 96 % and 99 % for a single and a double quantum well active structure respectively. Additionally, T_0 increased from 150K to 190K.

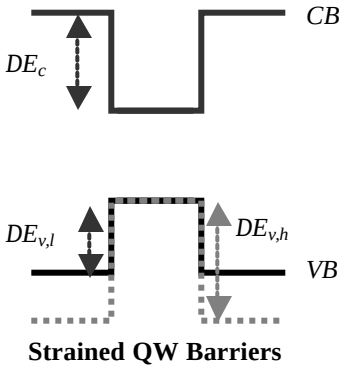

Figure 4 Schematic showing quantum well surrounded by strained barriers that introduce higher barriers for the holes due to lh-hh splitting.

As shown in Equation (1) reduction in V_0 also has a significant impact on peak power conversion efficiency. Our theory and simulation show that graded doping profile would lead to reduction in turn-on voltage as shown by the plot in the inset to Figure 5. A baseline structure (no SCH doping) and four structures with different SCH p-side doping profiles (constant, linear, super-exponential grade, and a 'spike' structure) were evaluated. These I-V curves were then fit to a model of a diode with a series resistor to determine V_0. There is a V_0 reduction of approximately 60mV between the undoped baseline structure and the spike-doped structure as shown in Figure 2. This would correspond to 4% improvement in power conversion efficiency.

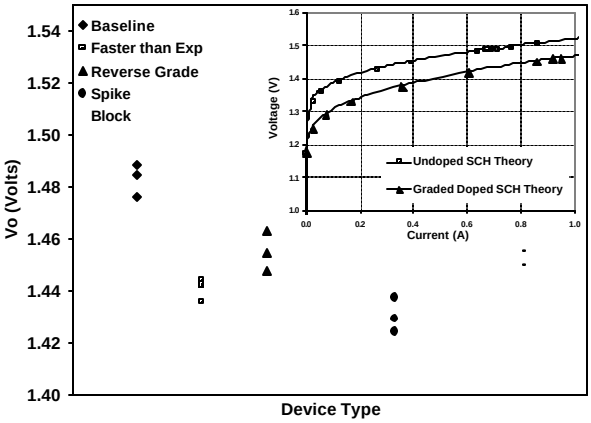

Figure 5 Measured Vo values as a function of p-side SCH doping profile and inset showing theoretical V-I predictions for graded doped and undoped SCH.

A theoretical analysis on the impact of built-in voltage, *Vo* and series resistance, *Rs* using compositional step between various heterostructure barriers was also studied. Each interface in the structure shown in Figure 1 was examined theoretically to determine its impact on *Vo* and *Rs*. The most important interfaces were found to be on the p-side due to its large theoretically predicted offset in the valence band.

Figure 6 shows theoretical results of statistically designed experiment. It shows results for the *Rs* and V_o as functions of the width and number of steps used between p-GaAs to p-InGaP interface. All of the modeling results are based on a 1um by 1um squares; allowing the results to scale with device geometry. The interfaces were modeled by applying 2V across the interface producing a theoretical I-V curve. From this I-V curve, the *Rs* and *Vo* were determined. We modeled step widths of 2nm, 6nm and 10nm and number of steps of 1, 4, and 7. The p-GaAs and p-InGaP were modeled at $1x10^{18}$ p-type carrier concentration. The studied showed largest reduction in V_o for 7 steps, each 10nm in thickness.

Figure 7 shows results for p-InGaP to p-Q1.62eV interface. We modeled doping in SCH with results shown in this figure labeled as 1, 5 and 10 (where $1=1x10^{17}$, $5=5x10^{17}$ and $10=1x10^{18}$) for carrier concentration and number of steps of 0, 1, and 2. The thickness of the step was fixed at 10nm. The p-InGaP and p-Q1.62eV were modeled at $1x10^{18}$ p-type carrier concentration. This leads to a potential reduction in voltage of about 0.11 V, increasing the *Rs* about 116 ohms. If we assume a 1mm by 100um device, this is only a 1.16 mohm increase in *Rs*.

Based on our theoretical predictions, we have also optimized the interface between the SCH and the cladding layers to reduce the turn-on voltage by 5%.

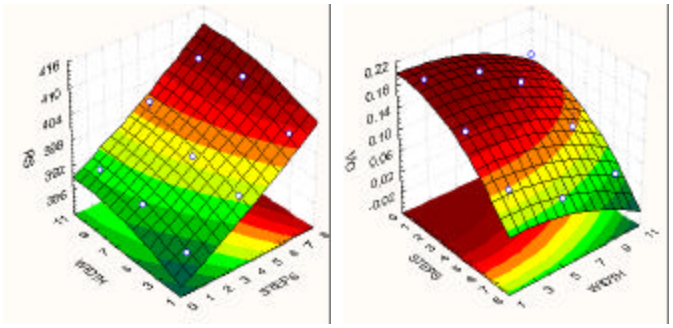

Figure 6 Designed response curves showing series resistance, R_s and built-in voltage, V_0 as a function of width and number of steps between p-GaAs to p-InGaP interface.

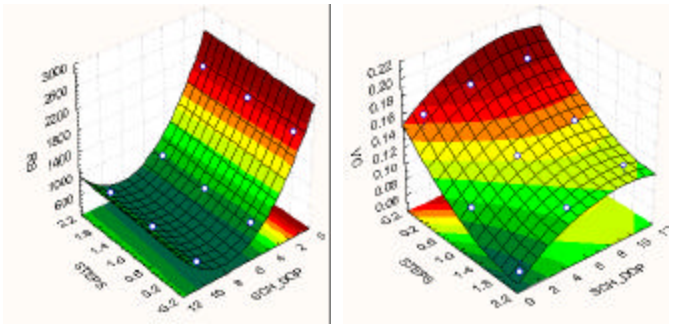

Figure 7 Designed response curves showing series resistance, R_s and built-in voltage, V_0 as a function of width and number of steps between p-InGaP to p-Q1.62eV interface.

Using aforementioned features to optimize both the external differential quantum efficiency and the turn-on voltage, we grew laser structure and fabricated into 1cm long bars with 1mm cavity length. As a result, we were able to achieve a record high power conversion efficiency of 70% near 970 nm wavelength at a heatsink temperature of 25C as shown in Figure 8. The laser diode bar operated with a slope efficiency of 1.12 W/A and threshold current of 4A.and a turn-on voltage of 1.303 V.

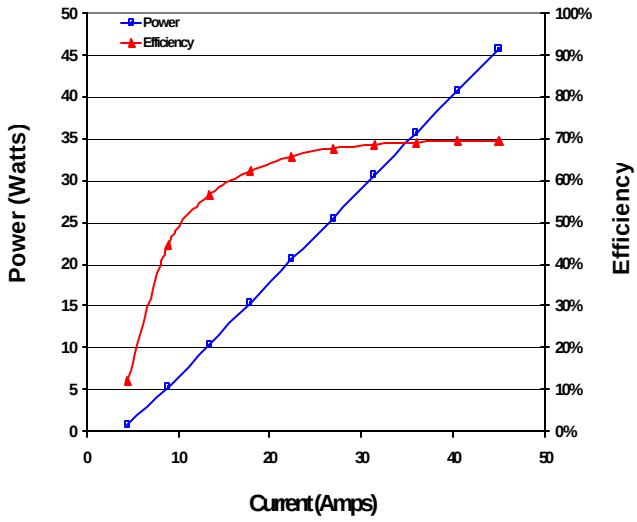

Figure 8 Plot showing CW L-I and 70% power conversion efficiency from 1cm long 970nm bar at 25C.

CONCLUSIONS

Due to increase in injection efficiency, judicious choice of doping of the SCH and heterostructure bandgap engineering we have achieved a record high power conversion efficiency of 70% for a 1cm bar at 25C. Further optimization is underway and we expect additional power conversion efficiency improvement due to decrease in losses from series resistance, threshold current, carrier leakage outside the active region, free-carrier absorption and mirror loss.

Acknowledgement: This work has been funded by DARPA-MTO under MDA972-03-9-0002 Super High Efficiency Diode Sources Program.

REFERENCES

[1] D. Botez, L.J. Mawst, A. Bhattarcharya, J. Lopez, J. Li, T.F. Kuech, V.P. Iakovlev, G. I. Suruceanu, A. Caliman, and A. V. Syrbu, *Electronics Letters*, 32, 2012 (1996).

[2] A. Al-Muhanna, L.J. Mawst, D. Botez, D.Z. Garbuzov, R.U. Martinelli, and J. Connolly, *Appl. Phys Lett.*, 71, 1142 (1997).

[3] M. Kanskar, M. Nesnidal, S. Meassick, A. Goulakov, E. Stiers, Z. Dai, T. Earles, D. Forbes, D. Hansen, P. Corbett, L. Zhang, T. Goodnough, L. LeClair, N. Holehouse, D. Botez and L.J. Mawst, IEEE SPIE Proceedings for Novel In-Plane Semiconductor Lasers II, 4995, 196 (2003).

[4] T. Fukunaga, et al, Appl. Phys. Lett. 69, 248 (1996).

[5] J.K. Wade et al., Appl. Phys. Lett. 72, 4 (1998).

[6] Y.S. Chun, S.H.Lee, I.H. Ho, G.B. Stringfellow, J. of Crystal Growth, 174, 585(1997),.

[7] S.R. Kurtz, J.M. Olson, D.J. Friedman, A.E. Kibbler, S. Asher, J. of Electron. Materials, 23,431(1994).

[8] C. Geng, A. Moritz, S. Heppel, A. Muhe, J. Kuhn, P. Ernst, H. Schweizer, F. Phillipp, A. Hangleiter, F. Scholz, J. of Cryst. Growth, 170, 418 (1997).

[9] D.P. Bour and A. Rosen, Journal of Appl. Phys., 66, 2813 (1989).

[10] L.J. Mawst, S. Rusli, A. Al-Muhanna, and J.K. Wade, IEEE J. Select. Topics Quantum Electron., 5, 785 (1999).